Engineering Dirhodium Artificial Metalloenzymes for Diazo Coupling Cascade Reactions

David M. Upp[1,†], Rui Huang[1,†], Ying Li[2], Maxwell J. Bultman[1], Benoît Roux[2,3,*], Jared C. Lewis[1,*]

[1]Department of Chemistry, Indiana University, Bloomington, IN 47405, USA
[2]Department of Biochemistry and Molecular Biology, University of Chicago, Chicago, IL 60637, USA
[3]Department of Chemistry, University of Chicago, Chicago, IL 60637, USA
[†]These authors contributed equally to this study.

Abstract

Artificial metalloenzymes (ArMs) are now commonly used to control the stereoselectivity of catalytic reactions, but controlling ArM chemoselectivity remains challenging. In this study, we engineer a dirhodium ArM to catalyze diazo cross-coupling to form an alkene that, in a one-pot cascade reaction, is reduced to an alkane with high enantioselectivity (typically >99% e.e.) by an alkene reductase. The numerous protein and small molecule components required for the cascade reaction had minimal effect on ArM catalysis, while the dirhodium cofactor itself provided only O-H insertion products from reaction with water and glucose under the same conditions. Directed evolution of the ArM led to improved yields and E/Z selectivities for a variety of substrates, which translated well to cascade reaction yields. MD simulations of ArM variants were used to understand the structural role of the cofactor on large-scale scaffold structural dynamics. These results highlight the ability of ArMs to control both catalyst stereoselectivity and chemoselectivity to enable reactions in complex media that would otherwise lead to undesired side reactions.

Introduction

The ability of transition metals to bind and react with a wide range of species underpins their utility as catalysts for diverse chemical transformations, but it also necessitates methods to ensure that a given metal species catalyzes a desired reaction at the correct site on a target substrate.[1] In the laboratory, this selectivity challenge is dramatically simplified by excluding all but the necessary components for a desired reaction. Transition metal chemoselectivity can then be tuned using ligands that modulate the steric and electronic properties of a metal center (its primary coordination sphere).[2] Significant effort has also been devoted to incorporating attractive substrate-catalyst interactions distal to a metal center (its secondary coordination sphere) to control catalyst selectivity.[3,4] Similar primary and secondary sphere effects are exploited by metalloenzymes to modulate transition metal reactivity,[5] and these examples have inspired many of the efforts to recapitulate enzyme-like secondary sphere effects in small molecule complexes[6].

The remarkable activities and selectivities of metalloenzymes are all the more impressive given that they operate in a complex cellular milieu. This capability suggests that the molecular recognition imparted by extensive and dynamic secondary sphere interactions enables far greater control over transition metal reactivity in metalloenzymes than can currently be achieved with small molecule ligands.[7] Similar control over synthetic metal complexes could enable reactions in complex environments, including enzymatic and chemoenzymatic cascades containing multiple catalysts, reagents, and intermediates.[8,9] Artificial metalloenzymes (ArMs) have been explored as a means to merge the reactivity of synthetic catalysts with the selectivity and evolvability of protein

scaffolds.[10] Moreover, streptavidin-,[11,12] LmrR-,[13] and albumin-based[14] ArMs have been used for *in vivo* catalysis, and streptavidin-,[15] FhuA-,[16] and P450-based[17] ArMs have been used for *in vitro* cascade reactions. In each of these examples, however, the inherent reactivity of the metal cofactors examined alleviates the need for scaffold controlled chemoselectivity. The ArMs produce the same products as the metal cofactors alone, albeit with impressive rate acceleration and enantioselectivity.

Our group has explored the design[18] and evolution[19] of dirhodium ArMs comprised of a bicyclononyne-substituted dirhodium cofactor (**1**)[20] covalently linked to *Pyrococcus furiosus* (*Pfu*) prolyl oligopeptidase scaffold containing a genetically encoded azidophenylalanine (Z) residue (Figure 1A). Dirhodium complexes react with donor-acceptor diazo compounds to generate highly reactive carbene complexes that, in turn, react readily with nucleophiles including water, thiols, amines, olefins, silanes, and even sp^3 C-H bonds.[21,22] We envisioned that this promiscuous reactivity would allow studies on the extent to which a protein scaffold, rather than reaction conditions or even the primary coordination sphere, can be engineered to control transition metal chemoselectivity. Indeed, previous studies in our laboratory established that ArM chemoselectivity can be evolved to favor carbene addition to olefins (i.e. cyclopropanation) over undesired formal insertion into water O-H bonds.[18] We also reasoned that this level of control over dirhodium reactivity could enable cascade reactions involving a variety of additional species in solution. For example, dirhodium-catalyzed diazo cross-coupling has been used to generate fumaric acid esters that are converted by alkene reductases to 2-substituted succinate derivatives (Scheme 1B).[23] In this study, however, dirhodium catalysis was conducted in organic solvent at cryogenic temperatures, and following this step, the solvent was evaporated and the residue dissolved in aqueous buffer to enable biocatalytic reduction. Herein, we evolve a dirhodium ArM that catalyzes diazo coupling with high chemo- and stereoselectivity and demonstrate that the resulting ArM can be interfaced with an alkene reductase in a one-pot cascade reaction to produce substituted succinate derivatives with high enantioselectivity (Scheme 1C).
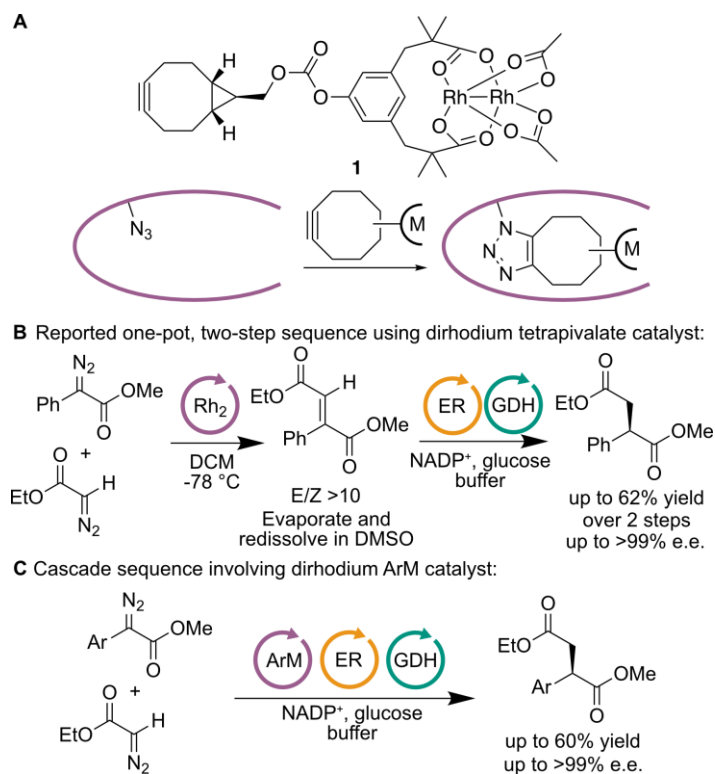
Figure 1. Dirhodium ArM formation and catalysis. A) Cofactor **1** and covalent bioconjugation strategy using genetically incorporated azidophenylalanine. B) Synthesis of chiral aryl succinates through previously reported one-pot, two-step reaction.[23] C) POP-**1**/ER cascade catalysis.

Results and Discussion

ArM Directed Evolution

The reactivities and selectivities of several previously-evolved dirhodium ArMs were first evaluated using a model diazo coupling reaction (Entries 1-3, Table 1). Because the ene reductases investigated are specific for the *E*-alkenes,[23] it was important to establish whether ArMs could provide the desired isomer in good yield under conditions suitable for biocatalysis. ArM variant 0-ZA$_4$ catalyzed diazo coupling with 46% yield and a 2.9:1 *E/Z* ratio (**4/5**), while variant 3-VRVH, the most evolved variant from our cyclopropanation lineage,[19] provided a 53% yield and 3.5:1 *E/Z* ratio. Variant 1-SGH,[19] which contains only the three mutations in 3-VRVH that are necessary for the high selectivity of the latter, provided a similar yield and *E/Z* ratio as 3-VRVH, so reaction conditions were optimized using this ArM. ArM loading could be reduced to 0.1 mol% with minimal change in yield, but excess **3** was required (Table 1, Entries 4 and 5, Table S1). We previously established that high salt concentrations are required for high ArM activity and selectivity,[18] and 0.7 M NaBr was sufficient in this regard (Entries 4, 6, and 7). Finally, THF and dioxane were found to be suitable co-solvents for the diazo coupling reaction. In all cases, the observed selectivity is substantially lower than that typically observed for the analogous reaction in organic solvent under cryogenic conditions (>10/1)[23], so improving this was a key goal of directed evolution. A significant amount (39%) of the donor-acceptor diazo substrate reacted with water, forming OH insertion product **6**, so minimizing this side reaction would also be required as in our previous evolution efforts[18,19].

Table 1. Scaffold selection and reaction optimization.[a]
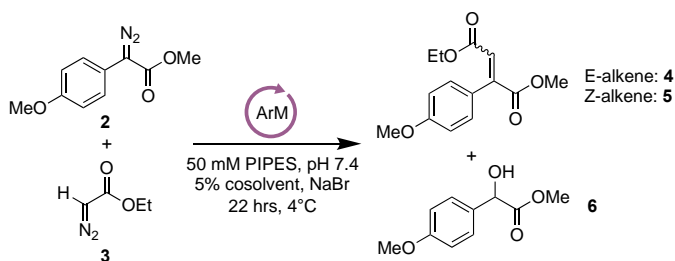
| Entry[a]	ArM Variant	[ArM] (μM)	[NaBr] (M)	Co-solvent	% Yield[c]			E/Z
					4	**5**	**6**	
1	ZA₄	50	0.7	THF	34	12	48	2.9
2	3'-VRVH	50	0.7	THF	41	12	35	3.5
3	1-SGH	50	0.7	THF	43	13	39	3.3
4	1-SGH	5	0.7	THF	44	12	31	3.7
5[b]	1-SGH	5	0.7	THF	39	13	37	3.1
6	1-SGH	5	0.1	THF	34	19	13	1.8
7	1-SGH	5	1.75	THF	46	8	33	5.7
8	1-SGH	5	0.7	Dioxane	46	11	42	4.2
9	1-SGH	5	0.7	DMSO	30	20	34	1.5

[a] Standard reaction conditions: 5 mM **2**, 25 mM **3**, 50 mM PIPES pH 7.4, 5% cosolvent, 22 hours at 4°C with shaking. [b] Standard conditions using 5 mM **3**. [c] Determined by SFC analysis using 1,3,5-trimethoxybenzene as internal standard. Reported yields and E/Z values are the average of triplicate reactions.

ArM evolution was conducted similarly to our earlier efforts.[19] Scaffold libraries containing the Z-477 mutation were expressed in 96-well plates and covalently modified in lysate using cofactor **1**. The resulting ArMs were immobilized on Ni-NTA resin in filter plates in which the diazo coupling reactions were conducted. Following reaction, the catalyst was removed by centrifugal filtration and the reaction products were analyzed by SFC. Previous efforts[18,19] revealed that mutations in a β-strand directly across the active site cavity from the presumptive Rh-binding histidine residue significantly impacted ArM-catalyzed cyclopropanation activity and selectivity. Site-saturation libraries were therefore constructed for several residues (98-101) in this β-strand of 1-SGH using degenerate NNK codons. This effort revealed that Q98P significantly improved the yield of **4**, increased the *E/Z* ratio, and decreased the yield of **6** (variant 2-P, Table 2). Site-saturation mutagenesis of F99 in 2-P led to the identification of variant 3-H (Table 2), which possessed a similar yield as 2-P but increased *E/Z* selectivity.

Similar mutagenesis of residues F100 and T101 did not lead to further improvements in ArM activity or selectivity. Combinatorial codon mutagenesis (CCM)[24] of 25 active site residues projecting into the active site of 3-H was therefore conducted using degenerate NDT codons. The mutation V71G (4-G, Table 2) was identified using this approach, but a subsequent CCM library

did not yield a positive variant. A subset of the residues in the CCM library were analyzed in more depth using site saturation (NNK) libraries, resulting in variant 5-G (E283G, Table 2), which displayed further improvements in diazo coupling yield and selectivity. Decreasing the ArM loading 100-fold from 0.1 mol% (5 μM) with respect to **2** to 0.001 mol% (50 nM) was found to substantially increase the TTN, with 5-G catalyzing 44,612 turnovers to **4**. If turnovers associated with formation of **5** and **6** are included, a remarkable 72,196 TTN is observed, highlighting the high activity of the dirhodium cofactor within 5-G.

Table 2. Directed evolution of ArM for diazo coupling.
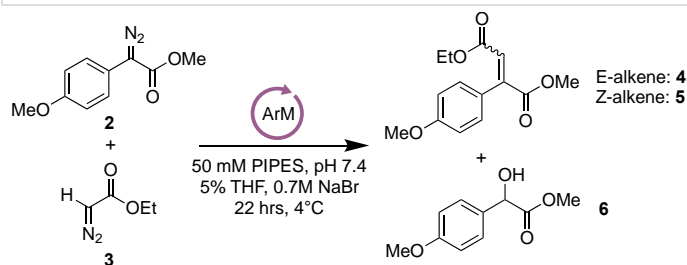
Entry[a]	Variant	Muta-genesis method	Mutations from previous generation	% Yield[c] 4	5	6	E/Z	TTN of **4**
1	1-SGH	-	Parent	44	12	31	3.7	388
2	2-P	Q98NNK	Q98P	55	11	33	4.9	545
3	3-H	S99NNK	S99H	51	7	24	7.3	511
4	4-G	CCM	V71G	72	8	21	8.6	717
5	5-G	CCM	E283G	76	6	16	13.3	761
6[b]	5-G	CCM	E283G	45	16	11	2.8	44612

[a] Standard reaction conditions: 0.1 mol% ArM, 5 mM **2**, 25 mM **3**, 50 mM PIPES pH 7.4, 5% THF, 22 hours at 4°C with shaking. [b] Standard conditions using 0.001 mol% (50 nM) ArM and 96 hour reaction time at 4 °C with shaking. [c] Determined by SFC analysis using 1,3,5-trimethoxybenzene as internal standard. Reported yields and E/Z values are the average of triplicate reactions.

The substrate scope of the evolved 5-G ArM was next evaluated under optimized reaction conditions. Improved yields of the desired *E*-alkenes were observed in all cases using 5-G relative to variant 1-GSH (Table 3), indicating that mutations accumulated during directed evolution generally improved the scaffold for diazo coupling. Steric and electronic perturbation of the aryl diazoacetate coupling partner (R1 and R2) were well tolerated, and both ethyl diazoesters and amides could be used (R3). With the exception of the previously unreported amide substrate, these substrates are in line with the known scope for dirhodium catalyzed diazo coupling,[23,25] indicating that the ArM enables the desired dirhodium activity while significantly reducing undesired side reactions such as water O-H insertion.

Table 3. Substrate scope of ArM-catalyzed diazo cross-coupling.

Entry[a]	R[1]	R[2]	R[3]	% Yield[b] 1-GSH	5-G
1	OMe	OMe	OEt	44	75
2	H	OMe	OEt	38	75
3	Cl	OMe	OEt	23	68
4	Br	OMe	OEt	38	73
5	OMe	OMe	NEt$_2$	33	58
6	OMe	OMe	OBn	18	34
7	Cl	Me	OEt	30	66

[a] Standard reaction conditions: 5 mM donor-acceptor diazo, 25 mM acceptor-only diazo, 50 mM PIPES pH 7.4, 0.7M NaBr, 5% THF, 22 hrs at 4°C with shaking. [b] Determined by HPLC analysis using 1,3,5-trimethoxybenzene as internal standard. Reported yields are the average of triplicate reactions.

ArM/ER Cascade Catalysis

The potential to leverage ArM substrate scope for the synthesis of enantioenriched succinate derivatives via cascade catalysis involving an ER was then explored. The activities of several ERs,[26,27] including alkene reductase from *Yersinia bercovieri* (YersER), enoate reductase 1 from *Kluyveromyces lactis* (KYE1) and 1,2-oxophytodienoate reductase from *Lycopersicum esculentum* (OPR1) were evaluated on the 2-aryl fumaric acid derivatives produced via ArM catalysis to select the optimal ER for each substrate (Table S2). Importantly, the ArM/ER cascade requires that the ArM, the ER, and a glucose dehydrogenase (GDH, needed to supply the ER with reduced cofactor) all tolerate one another, in addition to glucose, a terminal reductant that is converted to gluconic acid, and NADP(H). This challenge is particularly notable given that dirhodium carbenoid species react readily with water, proteins,[28] and a range of small molecule nucleophiles,[21] all of which would decrease cascade yields. Remarkably, however, the ArMs evaluated catalyzed desired diazo coupling with only slightly reduced yields even in the presence of all cascade components, and the ERs successfully converted the fumaric ester intermediates to the reduced products in good yields (Table 4). Under these conditions, 5-G catalyzed the desired alkene formation with a turnover number of up to 723, again highlighting the capacity of the ArM scaffold to protect the dirhodium center from deactivation and side reactions.

Table 4. Substrate scope of ArM/ER cascade reactions.
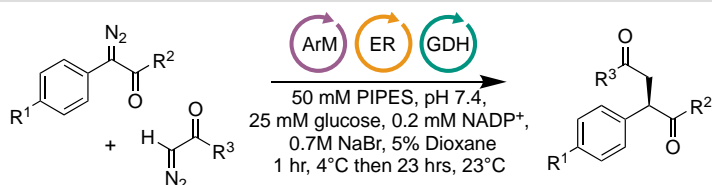
Entry[a]	ER	R[1]	R[2]	R[3]	% Yield[b] (e.e)[c]	
					1-GSH	5-G
1	KYE1	OMe	OMe	OEt	25 (>99%)	61 (>99%)
2	YersER	H	OMe	OEt	35 (>99%)	56 (>99%)
3	YersER	Cl	OMe	OEt	18 (>99%)	47 (>99%)
4	YersER	Br	OMe	OEt	32 (>99%)	60 (>99%)
5	OPR1	OMe	OMe	NEt$_2$	22 (>99%)	40 (>99%)
6	OPR1	OMe	OMe	OBn	6 (>99%)	10 (>99%)
7	YersER	Cl	Me	OEt	34 (79%)	52 (78%)

[a] Standard reaction conditions: 5 mM donor-acceptor diazo, 25 mM acceptor-only diazo, 50 mM PIPES pH 7.4, 0.7M NaBr, 5% dioxane, 1 hr at 4°C with shaking followed by 23 hrs shaking at 23 °C. [b] Determined by HPLC analysis using 1,3,5-trimethoxybenzene as internal standard. Reported yields are the average of triplicate reactions. [c] Enantioselectivity determined by chiral HPLC analysis.

The yield of the final succinic acid derivatives tracked with the ArM alkene yields (incomplete reduction by the ER was observed in Entry 6), suggesting that while the mutations gained throughout evolution increased diazo coupling performance, tolerance to cascade conditions was present from the outset of ArM evolution. On the other hand, diazo coupling reactions catalyzed by an acetyl-substituted cofactor in aqueous buffer provided the OH insertion product **6** almost exclusively and only trace **4** or **5** (Table S3). Moreover, in the presence of glucose, formal OH insertion involving both water and glucose was observed by mass spectrometry, but the latter is completely absent in the ArM catalyzed reaction (Figure S1). Finally, while dirhodium catalysts are capable of modifying surface-exposed cysteine and tryptophan residues on proteins under certain conditions,[28] no such modifications were observed by mass spectrometry for the ERs or GDH used in the cascade reactions. Together, these results are consistent with the ArM providing a hydrophobic environment for dirhodium catalysis that excludes polar nucleophiles like glucose and water to enable selective diazo coupling.[29]

ArM Conformational Dynamics

To gain insight into how the POP scaffold might give rise to the observed ArM selectivity, MD simulations were conducted on models of 5-G that involved different starting coordination states of dirhodium cofactor **1**. We previously reported that apo-POP undergoes large-scale domain opening and closing, where interdomain angles above 23° are considered open due to formation of a solvent-exposed cleft,[30] and similar behavior was observed for apo-5-G (Figure 2A, B). We speculated that analogous conformation dynamics in POP ArMs would facilitate cofactor bioconjugation in the open state and provide a more compact, hydrophobic environment conducive to selective catalysis in the closed state.[7] We further hypothesized that the improved selectivity of

ArMs containing specific active site His residues, such as H326 in 5-G, might result from an internal cross-link[31] favoring the closed form of the ArM. Supporting this notion, a MD simulation of a model of 5-G with the Rh-His bond intact revealed that the previously observed open/closed POP dynamics were greatly reduced (Figure 2C). Despite its flexible linker, cofactor **1** is able to staple 5-G closed when the Rh-His bond is present (Figure 2D). Interestingly, a simulation that started from a state lacking a Rh-His bond was able to access an open structure for much of the simulation (676/1000 ns, Figure 2D), though this system did not open to the same extent as apo 5-G. This constraint appears to result from a persistent hydrophobic interaction between **1** and a number of residues on the interior surface of the 5-G scaffold (Figure S2). This finding could explain the improved selectivity of POP-based ArMs lacking an interior His mutation,[18,19] but further free energy calculations and experimental validation will be required to establish this possibility.
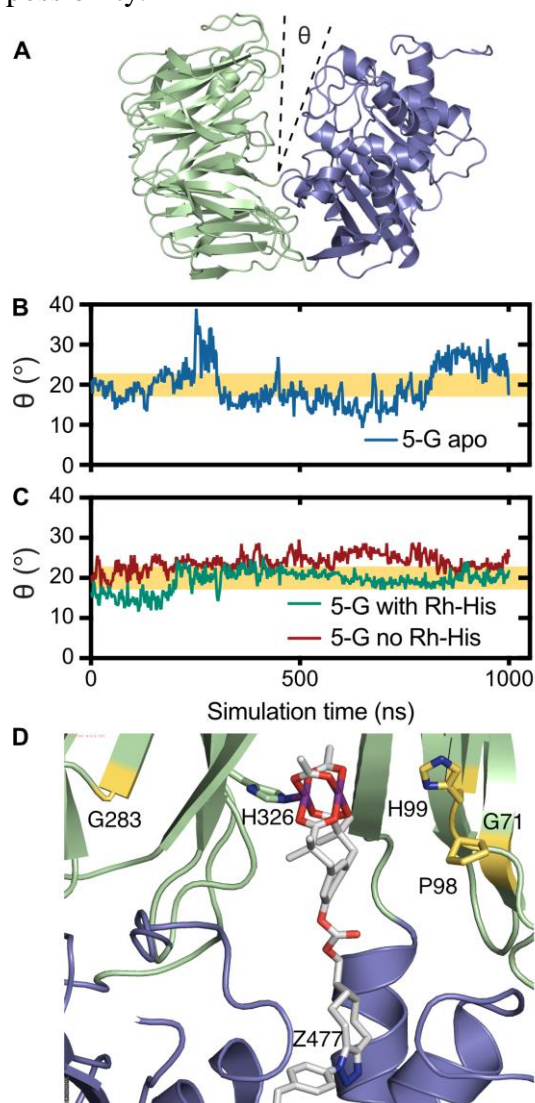

Figure 2. Domain dynamics of apo-POP and POP-**1** ArMs. A) Open state of apo-5-G showing the interdomain angle, θ. B) The interdomain angle of apo-5-G during a 1000 ns trajectory. The yellow bar (17-23°) indicates the open/closed transition. C) The interdomain angle of 5-G-**1** with (green)

and without (red) the parameterized Rh-His bond over a 1000 ns simulation. D) Representative trajectory showing the rhodium-histidine interaction in 5-G.

Conclusion

Controlling the reactivity and selectivity of a transition metal catalyst requires the precise tuning of its primary and secondary coordination sphere. The numerous potential interactions that can occur between a metal catalyst, a substrate, and an enzymatic scaffold make ArMs a promising platform for selective catalysis.[10] In this study, we showed that dirhodium ArMs can make use of first and second sphere interactions to catalyze diazo cross-coupling reactions in complex cascade reaction mixtures. Others have established that ArM scaffolds can help protect catalysts from poisons such as glutathione, which can reversibly bind to and deactivate metal centers,[11,14] but the current study highlights rare examples in which the chemoselectivity of a catalyst is modulated. Building on earlier observations for water tolerance by dirhodium ArMs,[18,19] this capability enables selective reaction of one functional group over many others on different substrates in solution, presumably by regulating substrate access to and orientation within the ArM active site. Previously evolved ArM variant 1-SGH was submitted to further directed evolution to improve diazo coupling yield and selectivity, increasing the yield of the desired E-alkene over the Z-alkene and OH insertion side products. These improvements were found to carry over to the cascade reaction with an ER. While it is likely that most of the four mutations found in this study are involved in outer-sphere control and substrate positioning, H326 and H99 have the possibility of binding directly to the rhodium atoms, anchoring it in place. This interaction was found to have significant effects on the dynamics of the scaffold in MD simulations, helping it to maintain a closed state when the rhodium-histidine interaction was enforced in simulations. These models suggest that there are a number of mechanisms by which the cofactor can affect the structural dynamics of the ArM scaffold, adopting dual catalytic and structural roles just as natural metalloenzyme cofactors do[32]. Further studies on this system will help clarify the different roles that cofactor-scaffold interactions can give rise to emergent properties in ArMs.

Acknowledgements

References

1. Afagh, N. A. & Yudin, A. K. Chemoselectivity and the Curious Reactivity Preferences of Functional Groups. *Angewandte Chemie International Edition* **49**, 262–310 (2010).

2. Mahatthananchai, J., Dumas, A. M. & Bode, J. W. Catalytic Selective Synthesis. *Angewandte Chemie International Edition in English* **51**, 10954–10990 (2012).

3. Knowles, R. R. & Jacobsen, E. N. Attractive Noncovalent Interactions in Asymmetric Catalysis: Links Between Enzymes and Small Molecule Catalysts. *Proceedings Of The National Academy Of Sciences Of The United States Of America* **107**, 20678–20685 (2010).

4. Toste, F. D., Sigman, M. S. & Miller, S. J. Pursuit of Noncovalent Interactions for Strategic Site-Selective Catalysis. *Accounts Of Chemical Research* **50**, 609–615 (2017).

5. Ragsdale, S. W. Metals and their scaffolds to promote difficult enzymatic reactions. *Chemical Reviews* **106**, 3317–3337 (2006).

6. Breslow, R. Biomimetic chemistry and artificial enzymes: catalysis by design. *Accounts Of Chemical Research* **28**, 146–153 (1995).

7. Lewis, J. C. Beyond the Second Coordination Sphere: Engineering Dirhodium Artificial Metalloenzymes To Enable Protein Control of Transition Metal Catalysis. *Accounts Of Chemical Research* **52**, 576–584 (2019).

8. Köhler, V. & Turner, N. J. Cascades with multiple engineered and/or heterologously expressed enzymes in vivo or as whole cell reactions. *Chemical Communications* **51**, 450–464 (2014).

9. Denard, C. A., Hartwig, J. F. & Zhao, H. Multistep One-Pot Reactions Combining Biocatalysts and Chemical Catalysts for Asymmetric Synthesis. *ACS Catalysis* **3**, 2856–2864 (2013).

10. Schwizer, F. *et al.* Artificial Metalloenzymes: Reaction Scope and Optimization Strategies. *Chemical Reviews* **118**, 142–231 (2017).

11. Jeschek, M. *et al.* Directed evolution of artificial metalloenzymes for in vivo metathesis. *Nature* **537**, 661–665 (2016).

12. Liang, A. D., Serrano-Plana, J., Peterson, R. L. & Ward, T. R. Artificial Metalloenzymes Based on the Biotin–Streptavidin Technology: Enzymatic Cascades and Directed Evolution. *Accounts Of Chemical Research* **52**, 585–595 (2019).

13. Chordia, S., Narasimhan, S., Paioni, A. L., Baldus, M. & Roelfes, G. In Vivo Assembly of Artificial Metalloenzymes and Application in Whole-Cell Biocatalysis**. *Angewandte Chemie Int Ed* **60**, 5913–5920 (2021).

14. Eda, S. *et al.* Biocompatibility and therapeutic potential of glycosylated albumin artificial metalloenzymes. *Nat Catal* **2**, 780–792 (2019).

15. Köhler, V. *et al.* Synthetic cascades are enabled by combining biocatalysts with artificial metalloenzymes. *Nature Chemistry* **5**, 93–99 (2012).

16. Mertens, M. A. S. *et al.* Chemoenzymatic cascade for stilbene production from cinnamic acid catalyzed by ferulic acid decarboxylase and an artificial metathease. *Catal Sci Technol* **9**, 5572–5576 (2019).

17. Huang, J. *et al.* Unnatural Biosynthesis by an Engineered Microorganism with Heterologously Expressed Natural Enzymes and an Artificial Metalloenzyme. (2021) doi:10.21203/rs.3.rs-130318/v1.

18. Srivastava, P., Yang, H., Ellis-Guardiola, K. & Lewis, J. C. Engineering a dirhodium artificial metalloenzyme for selective olefin cyclopropanation. *Nature Communications* **6**, 7789 (2015).

19. Yang, H. *et al.* Evolving artificial metalloenzymes via random mutagenesis. *Nature Chemistry* **10**, 318–324 (2018).

20. Yang, H., Srivastava, P., Zhang, C. & Lewis, J. C. A General Method for Artificial Metalloenzyme Formation through Strain-Promoted Azide–Alkyne Cycloaddition. *ChemBioChem* **15**, 223–227 (2014).

21. Gillingham, D. & Fei, N. Catalytic X–H insertion reactions based on carbenoids. *Chem Soc Rev* **42**, 4918–4931 (2013).

22. Davies, H. M. L. & Morton, D. Guiding principles for site selective and stereoselective intermolecular C–H functionalization by donor/acceptor rhodium carbenes. *Chemical Society Reviews* **40**, 1857–1869 (2011).

23. Wang, Y., Bartlett, M. J., Denard, C. A., Hartwig, J. F. & Zhao, H. Combining Rh-Catalyzed Diazocoupling and Enzymatic Reduction To Efficiently Synthesize Enantioenriched 2-Substituted Succinate Derivatives. *ACS Catalysis* **7**, 2548–2552 (2017).

24. Belsare, K. D. *et al.* A Simple Combinatorial Codon Mutagenesis Method for Targeted Protein Engineering. *ACS Synthetic Biology* **6**, 416–420 (2017).

25. Hansen, J. H. *et al.* Rhodium(II)-Catalyzed Cross-Coupling of Diazo Compounds. *Angewandte Chemie Int Ed* **50**, 2544–2548 (2011).

26. Yanto, Y. *et al.* Asymmetric Bioreduction of Alkenes Using Ene–Reductases YersER and KYE1 and Effects of Organic Solvents. *Org Lett* **13**, 2540–2543 (2011).

27. Stueckler, C. *et al.* Stereocomplementary Bioreduction of α,β-Unsaturated Dicarboxylic Acids and Dimethyl Esters using Enoate Reductases: Enzyme- and Substrate-Based Stereocontrol. *Org Lett* **9**, 5409–5411 (2007).

28. Chen, Z. *et al.* Catalytic Protein Modification with Dirhodium Metallopeptides: Specificity in Designed and Natural Systems. *Journal of the American Chemical Society* **134**, 10138–10145 (2012).

29. Breslow, R., Bandyopadhyay, S., Levine, M. & Zhou, W. Water Exclusion and Enantioselectivity in Catalysis. **7**, 1491–1496 (2006).

30. Ellis-Guardiola, K. *et al.* Crystal Structure and Conformational Dynamics of Pyrococcus furiosus Prolyl Oligopeptidase. *Biochemistry* **58**, 1616–1626 (2019).

31. Ball, Z. T. Designing Enzyme-like Catalysts: A Rhodium(II) Metallopeptide Case Study. *Accounts Of Chemical Research* **46**, 560–570 (2013).

32. Valasatava, Y., Rosato, A., Furnham, N., Thornton, J. M. & Andreini, C. To what extent do structural changes in catalytic metal sites affect enzyme function? *J Inorg Biochem* **179**, 40–53 (2018).